December 2009 Volume 4 Issue 2

Trade Science Inc.

Physical CHEMISTRY
An Indian Journal

Full Paper

PCAIJ, 4(2), 2009 [44-52]

Kinetics of acid-catalyzed breakdown of π-bonds and formation of carbonium ions for heptene in wide-ranging concentrations of H_2SO_4

Lev G.Helfman, Vladimir V.Gridin, Israel Schechter*

Department of Chemistry and Institute of Catalysis Science and Technology, Technion - Israel Institute of Technology, Haifa 32000, (ISRAEL)

E-mail : israel@techunix.technion.ac.il

Received: 20th June, 2009 ; Accepted: 30th June, 2009

ABSTRACT

UV-absorption of heptene was studied for variable concentrations, C_A, of sulfuric acid. The kinetic analysis of the experimental results involves thermodynamic considerations of acidity function (H_0) and activities of acid solutions. The π-bond originated band nearby 200 nm is blue shifted for C_A < 40%. The corresponding extinction coefficient of this band, ε_{200}, sharply drops by a factor of 4 on passing from the aqueous solution of heptene (ε_{200} =1300) to about ε_{200} = 350 for the C_A = 2% case. Moreover, kinetic analysis of the data indicates a monotonic increase of ε_{200} to about 3000 nearby C_A = 60%. A sudden drop to zero is observed for ε_{200} in the concentration range between 60% and 80%. This is accompanied by the appearance of an absorption band nearby 300 nm. The corresponding extinction coefficient, ε_{300}, shows a gradual rise to about 2500 at the highest C_A studied (= 96%). A similar monotonic rise of ε_{200} to about 4000 was also observed for this range of acid concentrations. The order of kinetic processes abruptly changes from 1 (for C_A < 60%) to 2 (for C_A > 80%). These new results are discussed in relation to the well-known formation of carbonium ions and the breakdown of π-bonds.

INTRODUCTION

Extensive studies of olefins in acidic environment have provided both theoretical[1-3] and experimental[4,5] foundation for the chemistry of hypercarbon and carbonium ions.[1,2,6-9] The latter play important role in hydration of olefins as well as in dehydration of alcohols.[10]

Traditionally considered mechanisms for these structures involve formation of carbonium ions by entrapment of proton nearby the π-bond (or bonds) of olefine molecules with a consequent addition of anions. Virtually any textbook of organic chemistry could provide introductory guidelines for the most common encounters with such processes.[11]

However, kinetic studies of the deuterium substituted olefins in the low-concentrated acid solutions show no evidence for the free state of carbonium ions.[12] Nowadays, the so-called acid catalysis[13,14] requires considerations of various ways by which attachment of proton to olefins takes place. The exact structure of solvated proton was shown to be of utmost importance in acid catalysis.[15-18]

Many schemes have been suggested and tested in respect of ionization processes, charge transfer, attachment of ion-pairs as well as for incorporation of various complexes with both acid and water molecules.[1,3,13] The needs for separate considerations of low-concentration (LC) and high-concentration (HC) regimes for

proton solvation in sulfuric acid, non-aquatic H_2SO_4 as well as in super acids (such as BF_3, HF, etc.) have been widely recognized.[2,14]

In respect of LC, it has been shown that solvated protons require two molecules of H_2O to form the $H_5O_2^+$ structure.[19] In turn, in case of the rather weak organic bases, such complexes as, e.g., $(CH_3OH)_2H^+$ may successfully compete with $H_5O_2^+$ in forming solvated proton structures.[20] Infra-red studies conducted in the wide ranging concentration of H_2SO_4 have revealed such structural changes for solvated proton as from $H_5O_2^+$ through $H_2O{\bullet\bullet\bullet}H^+{\bullet\bullet\bullet}OSO_3H$[21] up to $HO_3SO{\bullet\bullet\bullet}H^+{\bullet\bullet\bullet}OSO_3H$[22], while going from LC towards HC (from 5% to 99%).

Solvated protons in HC regime were studied by (naming just a few techniques): NMR, IR-spectroscopy, UV-absorption and Mass-Spectroscopy methods.[1,2,6-9] For many of these researches H_2SO_4 as well as such super-acids as FSO_3H-SbF_5, SO_2-SbF_5, BF_3, HF-SbF_5 (and the like) have been employed. In particular, an application of Paramagnetic Resonance had helped to identify *tert*-heptyl cat ions[23] in HF-SbF_5. Reports on olefine polymerization were made for the thermally activated acid-catalysis studies conducted between 50 °C to 100 °C.[24] Relevant to our theme, a broad UV-absorbing band at 300 nm is known[5] to appear in olefines when these are subjected to the HC environment of H_2SO_4. This observation is also interpreted in terms of carbonium ions.[1,5] Due to a drastic increase of the extinction coefficient associated with this band suggestions as for employing this effect in tracing the π-bond containing organics were made.[5]

However, to the best of our knowledge no comparative kinetic studies of the π-bond related UV-absorption were reported for heptene when the acid concentration range is traversed through from LC towards HC regime of sulfuric acid. Various medium parameters (acidity function, aqueous activity, etc.) ought to influence the rate coefficients for the proton solvating schemes resulting, thus, in distinct UV-absorption features to be observed.

In this work we report isothermal kinetics of UV-absorption of heptene, studied for variable concentrations, C_A, of sulfuric acid. Our findings indicate that the order of the underlying processes, the extinction coefficients and the most-likely structure of solvated protons, all these experience quite dramatic changes upon crossing through from $C_A < 60\%$ to $C_A > 80\%$. Discussion of these new results in terms of formation of carbonium ions and the breakdown of π-bond is given.

EXPERIMENTAL PROCEDURES

Isothermal kinetic study of UV-absorption by heptene (Fluke) in various concentrations, C_A, of sulfuric acid (Fluke) was performed at 25 °C using a spectrophotometer (Hewlett Packard 8453). The concentration range for C_A covered by kinetic study was from 43% to 95 %. Rectified heptene was purified by distillation. Sulfuric acid was of analytical grade. Concentration of sulfuric acid was determined by acid-base titration (Alkalimetry). Solutions of the required concentration were prepared by weight and molarity of solutions was calculated using density of solvents at 25°C.

The reactant was introduced into an optical (quartz) cell in aqueous solution containing 0.03 mol/l heptene. The concentration of heptene in the experiments varied between 2×10^{-4} to 9×10^{-4} mol/l. Typical time periods for kinetic measurements were strongly C_A dependent and varied from as little as few hours to several weeks. For $C_A < 40\%$ the kinetics was speeded up by stirring. The latter was virtually unimportant for larger C_A.

RESULTS

Typical UV-absorbance spectra of heptene in apolar (hexane) and polar (acid) solvents are shown in Figure 1 and indicate that the 205 nm band obtained in hexane, as a rule, is blue shifted by approximately 10 nm, when compared with that in sulfuric acid. Such a π-bond originated band at 190-210 nm (observed in apolar solvents) experiences only minute shifts for $C_A <$ 40%. By definition, the absorbance is directly proportional to both the concentration of the light-absorbing reagent (hereon: heptene) and to the respective extinction coefficient of the bands involved. Hereafter these were either situated around 200 or 300 nm.

The corresponding extinction coefficient of the 200 nm band, labeled hereafter as ε_{200}, sharply drops by a factor of 4 on passing from the aqueous solution of heptene (ε_{200} =1300) to about ε_{200} = 350 for the C_A =

Full Paper

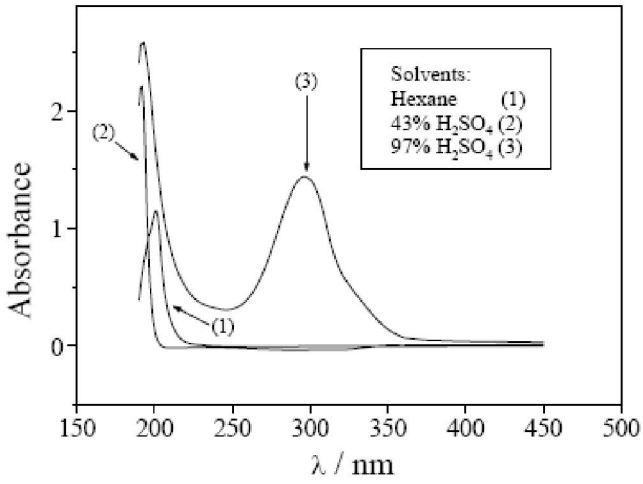

Figure 1 : Typical UV-absorbance of heptene in apolar (hexane) and polar (acid) solvents. Observe that the 205 nm band obtained in hexane, as a rule, is blue shifted by approximately 10 nm, when compared with that in sulfuric acid. Such a π-bond originated band at 190-210 nm (observed in apolar solvents) experiences only minute shifts for C_A < 40%. In high concentration regime the new band nearby 300 nm is well resolved.

2% case. Moreover, appearance of a distinct 300 nm band (also shown in Figure 1) is typical starting from $C_A \cong 70\%$; hereto the relevant ε_{300} extinction coefficient was obtained. The entire set of experimental values obtained for ε_{200} and ε_{300} is presented later on in this Section.

Kinetic analysis: Typical kinetic data (that is D = D(t)) for the peak-value absorbance, D_{200}, obtained in different concentration regimes for the 200 nm bands are shown in Figure 2a. Observe that the representative data gathered for the low concentration regime (LC; 43% < C < 60%) differs dramatically from that of the high-concentration (HC; 81% < C < 96%). Indeed, compare the monotonically vanishing D_{200} data of the LC regime to the gradually rising at HC. Different kinetic processes are immanent, hence, for describing such LC and HC results. This is further substantiated by the kinetic analysis presented, respectively, in Figure 2b and Figure 2c, for the representative LC and HC data sets.

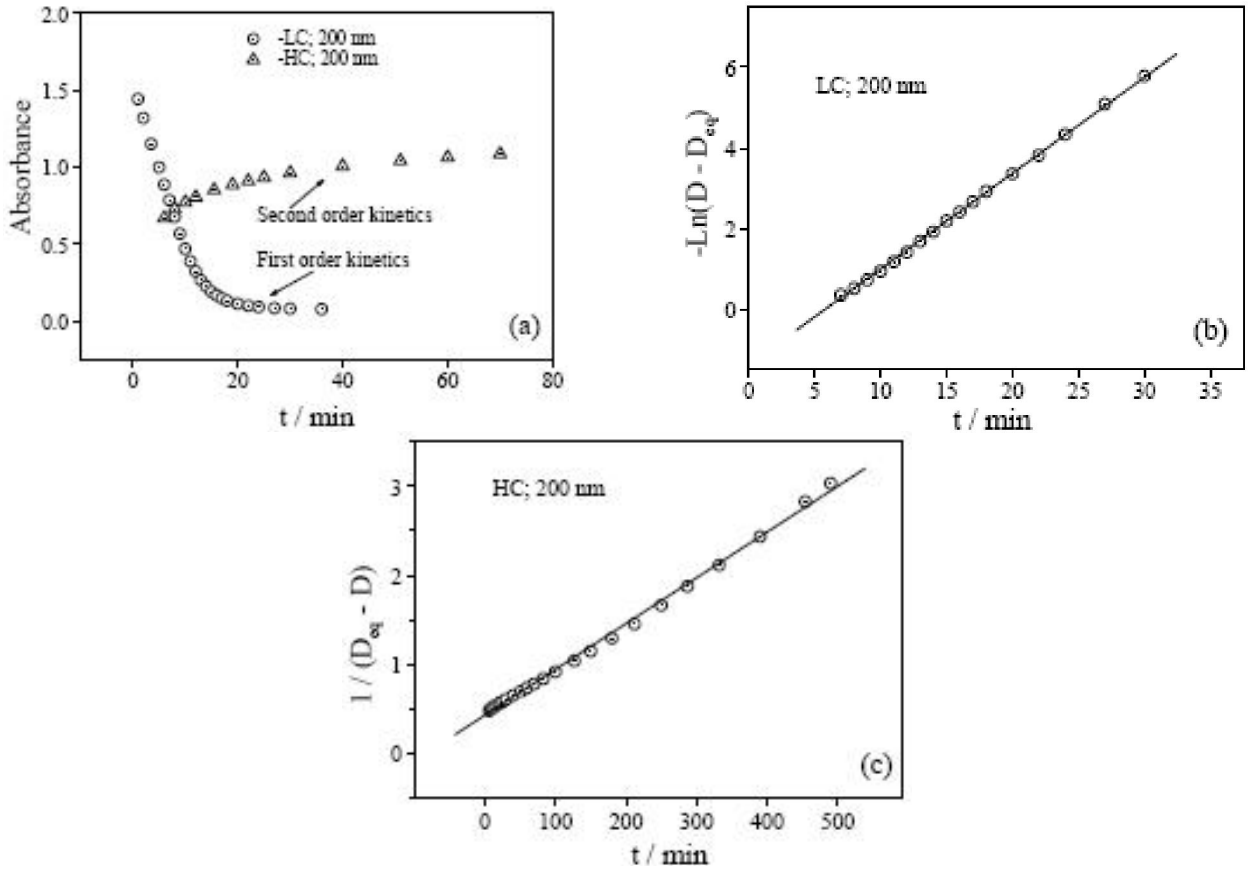

Figure 2 : (a) Typical kinetic data for absorbance, D, in different concentration regimes (LC; 43% <C < 60%) and (HC; 81% <C < 96%). Different kinetic processes are immanent for describing such LC and HC results. The representative kinetic analyses are exemplified in (b) for LC and in (c) for HC data sets.

By virtue of the data constructions shown in Figures 2b and 2c, the former case corresponds to the first order processes, while the latter is best fitted using the second-order data presentation approach.[3,6] In other words, provided that D = D(t), while D_{eq} stands for the absorbance figures obtained upon reaching the equilibrium conditions, the first order data presentation requires plotting Ln(D - D_{eq}) as a function of t. Recall that second-order processes are best analyzed by linearity of the 1/(D_{eq} –D) versus.

The corresponding rate constants for the processes in LC and HC regimes were derived from the respective linear regression fits shown in Figure 2b and Figure 2c. Hence, on passing through C_A = 60-80% the order of kinetic processes is abruptly changed from 1 (for C_A < 60%) to 2 (for C_A > 80%). The entire set of experimental findings is presented in TABLE 1.

For the LC regime the kinetic measurements allow for the initial (i.e., the maximal) values of extinction coefficients (via extrapolation of data in Figure 2b to t = 0) to be obtained. Kinetic analysis of the data indicates a monotonic increase of ε_{200} to about 3000 nearby $C_A \approx$ 60%.

It should be noted that for the HC regime the maximal figures for extinction coefficients were derived as the equilibrium readings in the respective UV-absorbance runs (held for about three weeks at 25 centigrade). Analysis of absorbance at 300 nm band also results in a second-order kinetic process, similar to that depicted in Figure 2c for the 195 nm (≈200 nm) band of such HC runs. A monotone rise of ε_{200} to about 4000 was observed for this range of acid concentrations.

Extinction coefficients are plotted in Figure 3 for the entire concentration range covered in this study. Several observations are worth summarizing:

TABLE 1 : Rate constants for the first and second order processes in acid-catalyzed decomposition of heptene and formation of carbonium ions.

CA	k_{eff} (x102) (min^{-1}) (First order) LC; 200 nm	k_{eff}*(x10^2) (min^{-1}) (First order) LC; 200 nm	k_{eff} $(mole/l)^{-1}min^{-1}$ (Second order) HC; 200 nm	k_{eff} $(mole/l)^{-1}$ min^{-1} (Second order) HC; 300 nm	α
43	0.44	0.225			0.8
44.4	0.58	0.276			0.9
45.7	0.69	0.487			2.5
48.6	1.10	1.06			13
51.2	2.20	2.0			12
53	4.87	4.17			6
54.5	9.58	9.05			16
56	10.70	10.2			34
56.2	12.80	12.4			29
56.9	19.50	18.0			21
57.6	23.80	23.3			32
58.6	29.40	28.4			30
85.1			1.6	2	
87.4			2	3	
89.9			3	9.5	
92.5			9	15	
94.8			18.4	22.60	
96.0			44	48	

C_A - concentrations of H2SO4, [%].

α = (C0 - Ceq) / Ceq; C0 and Ceq are the initial and the final (t→8) concentration of heptene; see text and Re: eq. 14.

k_{eff} – experimental rate constants; refer to Figures 2b, 2c and eqs. 7a, 7b; see also eqs. 8, 13.

k_{eff}* = αk_{eff} / (1 + α).

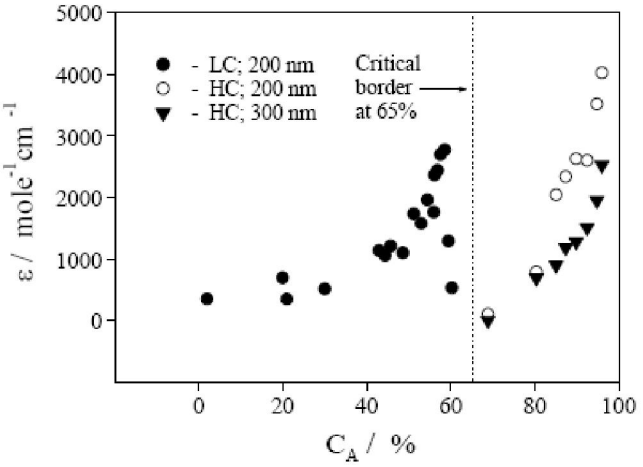

Figure 3 : Extinction coefficients for the bands specified in Figure 1. The data obtained from kinetic studies, as well as the equilibrium data (very slow, if any, time-dependence), are plotted for the entire concentration range covered in this study. Observe a vertical line drawn at 65%. Significance of such borderline and the experimental entries are detailed in text.

1. A sudden drop to zero is observed for ε_{200} in the concentration range between 60% and 80%.
2. The HC data of both ε_{200} and ε_{300} exhibit similar rise, though the absolute figure reached by ε_{300} at C = 96% are about 2/3 of that found for ε_{200}.
3. Moreover, it appears that the LC-rise of ε_{200} is similar to that obtained for ε_{200} and ε_{300} in the HC regime.
4. Observe a vertical line drawn at 65%. Significance of such boundary would be discussed in the forth-

coming section. It was verified that, while traversing this line by increasing (or decreasing) C_A, the above-listed HC (or LC) typical features of UV-absorption spectra were reproducibly recovered.

DISCUSSION

While inspecting the observations presented in Figures 1-3, it is clear that the radically different interpretations of experimental findings ought to be considered for the crossing over from LC to HC regime. This section is organized as follows: First, a general approach to kinetic analysis in terms of the thermodynamic values of acidity function (H_0) and activities of the acid solutions is given. Then, relevant mechanisms for reaction of heptene with sulfuric acid are separately considered for HC and LC regimes. An estimate of the borderline concentration (refer to Figure 3) concludes the section.

Thermodynamics of acid catalysis: Analysis of the base-acid equilibrium involves considering the Hammett's[3] acidity function, H_0. In particular, kinetics of the acid-catalyzed hydrolysis of ethers,[25-27] lactams,[28] dehydration of alcohols,[29-31] aldol addition reactions[3] and many others[13,14] have been successfully analyzed and interpreted this way.

Briefly speaking, H_0 was, at first, introduced for nitroanilines[32] in order to describe the reversible addition of proton to this group of compounds, via the generalized reaction:

$$B + H_3O^+ \Leftrightarrow BH_3O^+ \quad (1)$$

This type of processes was shown to be better-represented[13] by the equilibrium between:

$$B + H_5O_2^+ \Leftrightarrow BH_3O^+ + H_2O \quad (2)$$

Such processes allow a standard thermodynamic description using a formal definition of the acidity function. Indeed, let K_{eq} stand for the equilibrium constant of the processes in eq. (1), or eq. (2). The corresponding activities, labeled as a_B, a_{H3O+} and a_{BH3O+}, are readily defined via the appropriate molarity, C, and activity coefficients, f, by means of: $a_B = C_B f_B$ and $a_{BH3O+} = C_{BH3O+} f_{BH3O+}$. Let the degree of ionization, I, be defined as: $I = C_{BH3O+}/C_B$. In turn, the acidity, h_0, is introduced by means of $h_0 = a_{H3O+} f_B / f_{BH3O+}$. Then the equilibrium conditions require that:

$$K_{eq} = a_B\, a_{H3O+} / a_{BH3O+} \quad (3a)$$

or

$$K_{eq} = h_0 / I \quad (3b)$$

In other words, while labeling $pK = -Log(K_{eq})$ together with the definition of acidity function as $H_0 \equiv -Log(h_0)$, the thermodynamic description of the above processes is simply standardized. The validity of the linear relationship provided by:

$$H_0 = pK - Log(I) \quad (3c)$$

then ought to be verified for the specific reactants involved.

It should be noted, however, that there exists another ionization process that does not involve attachment of protons. This, for instance, is well-documented[33] for asulenes. The ionization mechanism proceeds by the attachment (addition) of an ionic-pair (acidic; labeled hereon as HA) via the following scheme:

$$B + HA \Leftrightarrow B \bullet HA \quad (4)$$

In such a case eqs. 3b and 3c are respectively replaced[14] by:

$$K_{eq} = a_{HA} / I \quad (5a)$$

and

$$Log(a_{HA}) = pK + Log(I) \quad (5b)$$

with the obvious redefinition of I to read as: $I = C_{B \cdot HA} / C_B$. General features of eqs. 3b-3c and eqs. 5a-5b are, respectively, employed in the forthcoming kinetic analysis of the data obtained for HC and LC regimes.

Mechanisms: Acidic catalysis is known[3,13] to proceed in a two-steps: (a) a fast, reversible ionization of B (refer to eqs. 1-2) and (b) a rate-limiting decomposition of reactive complexes (such as, e.g., BH_3O^+). In our case, the second irreversible step, whereby the products of reaction are obtained, is the one responsible for the decomposition of the π-bonds. Schematics of the events are:

$$B + H_5O_2^+ \Leftrightarrow BH_3O^+ + H_2O \rightarrow \text{Products} \quad (6)$$

As before, the equilibrium stage is characterized by K_{eq} of eq. 3a. In turn, for the decomposition of reactive complexes, the experimentally observed effective rate of reaction, v_{eff}, is assumed to coincide with the theoretically expected decomposition rate, v_{dec}. The former and the latter are, respectively,

$$v_{eff} = k_{eff} C_B \quad (7a)$$

and

$$v_{dec} = k_{act} C_{BH3O+} \quad (7b)$$

Hereafter, k_{eff} stands for the experimentally observed rate constant, whereas k_{act} corresponds to the, in general unknown, rate constant of the decomposition stage.

Worth-noting that v_{eff} corresponds to the entire sequence of events specified by eq. 6, whereby v_{dec} characterizes the rate-limiting decomposition step only. Upon equalizing $v_{eff} = v_{dec}$ and for the processes where eq. 3b is satisfied, one obtains:

$$k_{eff} = k_{act} h_o / K_{eq} \quad (8)$$

Hence, in accord with the relation:

$$Log(k_{eff}) = Log(k_{act} / K_{eq}) - H_0 \quad (9)$$

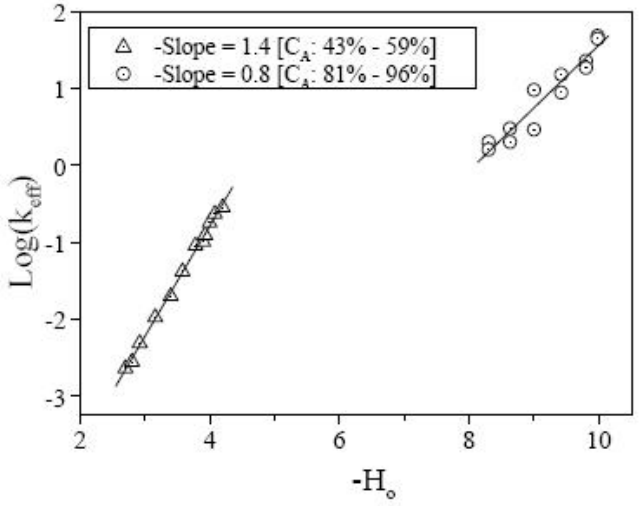

Figure 4 : Experimental data of keff for both LC and HC regimes (refer to TABLE 1) are plotted in accord with eq. 9. Observe that in the LC case the resulting slope value is nearly 1.4, whereas for HC it is smaller than unity and is roughly = 0.8.

A plot of $Log(k_{eff})$ as a function of $-H_0$ should produce a linear regression with the slope = 1. Experimental data for both LC and HC regimes (refer to TABLE 1) are plotted in Figure 4 according to eq. 9. Activities of water as well as that of acid were taken from literature.[34,35] For the acidity function, H_0, the results supplied by Johnson et al.[36] were used. Observe that in the LC case the resulting slope value is nearly 1.4, whereas for HC it is smaller than unity and is roughly = 0.8.

Such significant deviations from the theoretically anticipated slope value of 1 call for additional considerations[13,14] as for the exact thermodynamic parameters and mechanism that govern either of the above cases.

This approach differs from the more traditional one,[37,38] where the acidity functions were adjusted in order to force the slope value to the desired one. The reaction mechanism was kept unaltered in such cases. Following the more recent approach, however, we turn discussing the relevant mechanisms that would bring to unity the slope values of Figure 4.

To start with, we note that in certain cases,[10] the schematic presentation of acidic catalysis is known to differ from that of eq. 6 and, instead, follows the path:

$$B + H_5O_2^+ \Leftrightarrow (BH_3O^+)\bullet H_2O \rightarrow \text{Products} \quad (10\text{-I})$$

The relevant linear regression with slope = 1 would be then obtained in accord with

$$Log(k_{eff}) = Log(k_{act}/K_{eq}) + Log(h_0 a_{H2O}) \quad (11)$$

The left-hand-side of eq. 11 is plotted as a function of $Log(h_0 a_{H2O})$. Here the water activity is taken at the appropriate concentration of the generalized acid, HA.

HC regime: Using the construction suggested by eq. 11, the experimental data of k_{eff} in HC regime (refer to TABLE 1) are plotted in Figure 5a. The proximity to the "slope = 1" line of both sets of kinetic data obtained from 200 and 300 nm absorption bands is evident.

It might be argued, however, that the experimentally obtained second-order processes are in conflict with the first-order ones suggested by eq. 10-I. Such apparent discrepancy is readily removed, however, if a second-order process is proposed. Indeed, via introducing an additional, rate-limiting, collision of the complex $(BH_3O^+)\bullet H_2O$ with another B molecule:

$$B + H_5O_2^+ \Leftrightarrow (BH_3O^+)\bullet H_2O \quad (10\text{-IIa})$$

$$B + (BH_3O^+)\bullet H_2O \rightarrow \text{Products} \quad (10\text{-IIb})$$

the second-order process is readily recognized.[13] It could be shown that eq. 11 still holds, nonetheless.

Several modifications of the general process depicted by eqs. 10-II are in place for heptene and sulfuric acid. For $C_A > 80\%$ the introduction of heptene results in a fast stage during which the π-bond of heptene is broken resulting thus in $C_7H_{15}OSO_3H$ (heptyl hydrogen sulfate) or in heptanol.

Full Paper

At first the proton is solvated while giving rise to $H_2O\bullet\bullet\bullet H^+\bullet\bullet\bullet OSO_3H$. Then, upon increasing C_A a further replacement of water leads to $HO_3SO\bullet\bullet\bullet H^+\bullet\bullet\bullet OSO_3H$ complexes. For heptyl hydrogen sulfate, the reactive complex $(BH_3O^+)\bullet H_2O$ and the products of reaction become, respectively:

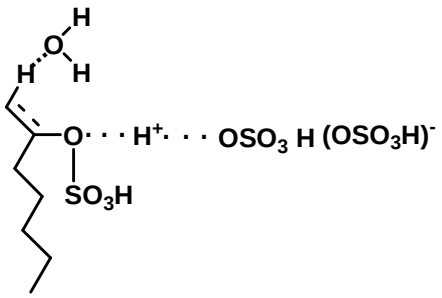

and

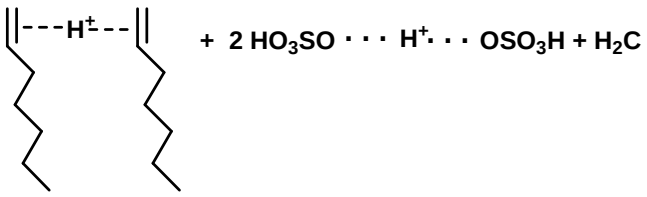

Note that a similar scheme could be readily suggested for heptanol. Observe that a pair of de-localized π-bonds appears as one of the products. Such de-localized π-bonds are responsible for the 200 nm absorption band as before.

On the other hand, the basic structure is similar to that of the well-documented carbonium ions,[6] for which the 300 nm band has been widely studied.[5-9] Note that the suggested form allows for both (a) the catalytic action of sulfuric acid and (b) the self-consistent interpretation of experimental data to be made.

In other words, the recovery of the 200 nm absorption and the kinetics of the 300 nm band suggest, both quantitatively (as is evident from the HC branch of Figure 3 and qualitatively (refer to Figure 5a), similar modifications of the corresponding density of states as a function of increasing C_A. Similar process-limiting route of eqs. 10-II seems to hold for them both. Let us turn discussing the LC regime.

LC regime: A fast reversible ionization should follow eq. 4. In such case B reacts with ionic-pair of acid HA. When the irreversible, rate-limiting step is included the entire process could be generalized as:

$$\mathbf{B + HA \Leftrightarrow B\bullet HA \rightarrow Products} \qquad \mathbf{(12)}$$

Then the procedure (similar to that described by eqs. 6, 7a and 7b) could be shown to produce:

$$\mathbf{k_{eff} = a_{HA} k_{act} f_{BHA} / K_{eq} f_B} \qquad \mathbf{(13)}$$

Since in our case HA = H_2SO_4, then, provided that f_{BHA}/f_B is independent of C_A, the relevant linear regression with slope = 1 would be obtained if, in accord with

$$\mathbf{Log(k_{eff}) = Log(k_{act} f_{BHA} / K_{eq} f_B) + Log(a_{HA})} \qquad \mathbf{(14)}$$

the left-hand-side of eq. 14 is plotted as a function of $Log(a_{HA})$.

Strictly speaking, eq.14 should be valid for the fully irreversible rate-limiting stage. Our experiments have revealed, however, that the decomposition of heptene's

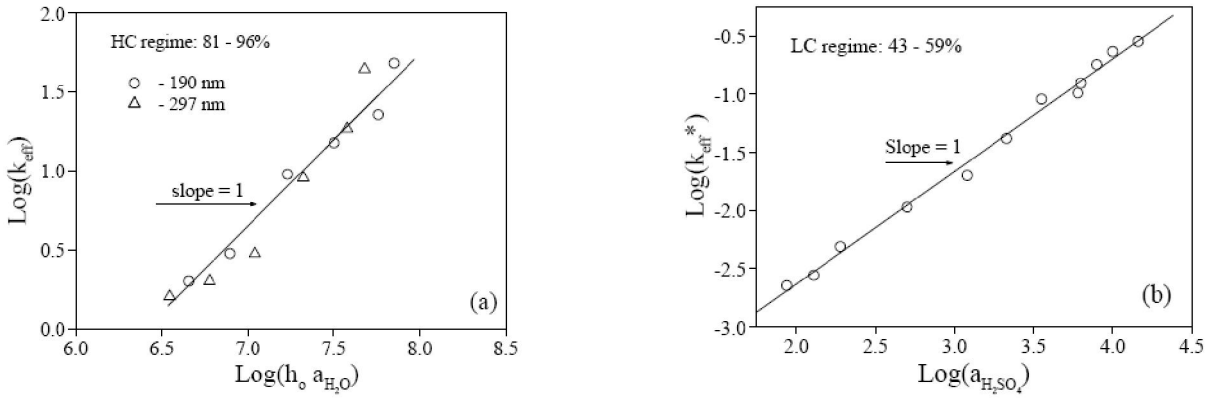

Figure 5 : Upon reconsidering the proton solvation complexes and the relevant mechanisms, the data of Figure 4 are replotted. In (a) the experimental data of k_{eff} in HC regime (refer to TABLE 1) is presented in accord with eq. 11; in (b) a similar construction as above is shown for k_{eff}* of the LC data sets (refer to eq. 14). The proximity to the "slope = 1" line of both sets of kinetic data obtained from 200 and 300 nm absorption bands (as for (a)) and from 200 nm band (as for (b)) is self-evident.

π-bond was, although irreversible, partially incomplete for $C_A < 46\%$.

To account for this effect let the degree of heptene decomposition, α, be defined as: $\alpha = (C_0 - C_{eq}) / C_{eq}$; here C_0 - is the initial concentration of heptene, and C_{eq} corresponds to that obtained at the equilibrium phase of kinetic measurements ($t \rightarrow 8$). The corrected value of k_{eff}, denoted as k_{eff}*, is defined[10] as $k_{eff}^* = \alpha k_{eff} / (1+\alpha)$. Values of k_{eff}, α and k_{eff}* are shown in TABLE 1. Figure 5b shows a plot of Log(k_{eff}*) as a function of Log(a_{HA}); observe that the "slope = 1" line agrees reasonably well with the data of this Figure. In our case, the reaction that

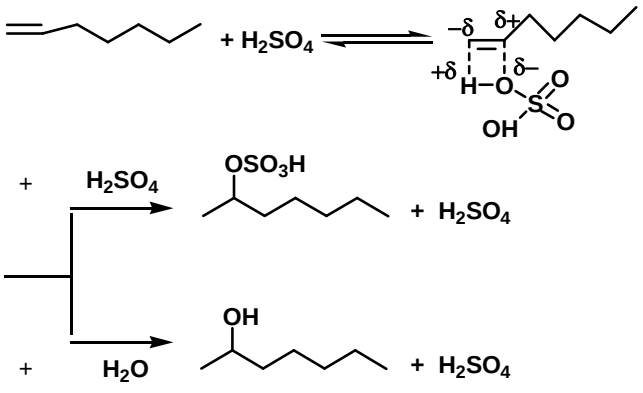

follows the general process depicted by eq. 13 is:

Here, the rate-limiting step is known to exist for olefines.[3,6,11] In accord with our kinetic results, the reversible charge separation step is assisted by attachment of the ion-pairs to heptene.

Critical boundaries: Stoichiometric calculations for dissociation of sulfuric acid suggest that below 57.6% the protons get solvated via two molecules of H_2O giving rise, thus, to $H_5O_2^+$. On the other hand, for $C_A \approx 73.1\%$ the deficit of water results at first in $H_2O{\bullet\bullet\bullet}H^+{\bullet\bullet\bullet}OSO_3H$ which is followed by formation of $HO_3SO{\bullet\bullet\bullet}H^+{\bullet\bullet\bullet}OSO_3H$ upon a further increase of C_A.

The critical boundary in Figure 3 was drawn midway of the above estimates at around 65%. It falls, roughly speaking, in between the concentration values suggested by the above noted proton-H_2O bonding structures. Very fast kinetics of the π-band decay occurs to its left. In turn, immediately to the right of this line a very slow (several weeks) recover of the π-band absorption, as well as a diminishing appearance of the 300 nm band, were recorded. Complementary methods could be envisaged to do better in this cross-over regime of sulfuric acid concentrations.

CONCLUSIONS

Kinetic study of UV-absorption by heptene in wide concentrations of sulfuric acid revealed a critical boundary for the acid catalysis mechanisms. These were suggested and reasonably well supported by experimental findings. The significance of thermodynamic considerations for proposing various catalytic routes was explored and involved recognition of different proton-solvation complexes. This way, the first- as well as second-order kinetics in respect of the low- and the high-concentrations of sulfuric acid were self-consistently accounted for. Most of the experimental findings are novel and offer challenging insights into catalytic action of sulfuric acid and the reaction schemes involved. Since the critical range of concentrations (between 60% to 80%) revealed here for the first time is rather poorly accessible by the method employed, further theoretical and experimental studies seem to be needed.

ACKNOWLEDGMENTS

L.G.F. and V.V.G. are grateful for financial support by The Center for Absorption in Science, Ministry of Immigrant Absorption, Israel. This research was supported, in part, by the James Frank Program in Laser Matter Interaction.

LITERATURE CITED

[1] George A.Olah, Paul von R.Schleyer, (Eds.); 'Carbonium Ions', v1: General Aspects and Methods of Investigation; Interscience Publishers-a division of John Wiley & Sons, Inc., New York, **(1968)**.
[2] George A.Olah, Paul von R.Schleyer, (Eds.); 'Carbonium Ions', v3: Major types (continued); Interscience Publishers-a division of John Wiley & Sons, Inc., New York, **(1972)**.
[3] Louis P.Hammett; 'Physical Organic Chemistry. Reaction rates, Equilibrium and mechanisms,' McGraw-hill book company, **(1970)**.
[4] J.Gonzales-Vidal, E.Kohn, F.A.Matsen; J.Chem. Phys., **25**, 181 **(1956)**.
[5] A.P.Altshuller, S.F.Sleva, A.F.Wartburg; Analytical Chemistry, **32**, 94 **(1960)**.

Full Paper

[6] George A.Olah, Paul von R.Schleyer, (Eds.); 'Carbonium Ions', v2: Methods of Formation and Major Types; Interscience Publishers-a division of John Wiley & Sons, Inc., New York, **(1970)**.
[7] George A.Olah, Paul von R.Schleyer, (Eds.); 'Carbonium Ions', v4: Major types (continued); Interscience Publishers-a division of John Wiley & Sons, Inc., New York, **(1973)**.
[8] George A.Olah, Paul von R.Schleyer, (Eds.); 'Carbonium Ions', v5: Miscellaneous Ions, theory and structure; Interscience Publishers-a division of John Wiley & Sons, Inc., New York, **(1976)**.
[9] George A.Olah, G.K.Surya Prakash, Robert E.Williams, Leslie D.Field, Kenneth Wade; 'Hypercarbon chemistry,' Wiley-Interscience Publications-John Wiley & Sons, Inc., New York, **(1987)**.
[10] M.I.Vinnic, P.A.Obraztsov; Usp.Chem., **59**, 106 **(1990)**.
[11] Graham Solomons, Craig Fryhle; 'Organic Chemistry,' John Wiley and Sons, Inc., **(2000)**.
[12] V.Gold, M.A.Kessik; J.Chem.Soc., 6718 **(1965)**.
[13] M.I.Vinnik; Kinet.Katal, **28**, 100 **(1987)**.
[14] M.I.Vinnik; Kinet.Katal, **21**, 136 **(1980)**.
[15] D.Marx, M.E.Tuckerman, Jurg Hutter, M.Parinello; Nature, **397**, 601 **(1999)**.
[16] Lars Ojamae, Isaiah Shavitt, Shervin J.Singer; J.Chem.Phys., **109**, 5547 **(1998)**.
[17] G.Zundel, H.Metzger; Z.Phisik.Chem.(N.F.), **58**, 225 **(1968)**.
[18] P.Schuster, G.Zundel; 'The hydrogen Bond-Recent Developments in Theory and Experiments,' North-Holland, Amsterdam., 683 **(1976)**.
[19] M.I.Vinnik, I.S.Kislina, N.B.Librovich; Dokl.Akad. Nauk SSSR [Phys.Chem.], **251**, 138 **(1980)**.
[20] D.Maiorov, G.I.Voloshenko, N.B.Librovich, M.I.Vinnik; Izv.Akad.Nauk, Ser.Khim., **10**, 2261 **(1992)**.
[21] V.D.Maiorov, N.B.Librovich, M.I.Vinnik; Izv.Akad.Nauk SSSR, Ser.Khim., **2**, 281 **(1979)**.
[22] I.S.Kislina, N.B.Librovich, M.I.Vinnik; Izv.Akad. Nauk SSSR, Ser.Khim., **11**, 2458 **(1985)**.
[23] see page 769 of ref. **[6]** above.
[24] see page 199 of ref. **[1]** above.
[25] N.B.Librovich, M.I.Vinnik; Zh.Fiz.Khim., **53**, 2993 **(1979)**.
[26] A.I.Smirnov, M.I.Vinnik; Zh.Fiz.Khim., **53**, 1247 **(1979)**.
[27] A.I.Smirnov, M.I.Vinnik; Zh.Org.Khim., **25**, 1920 **(1989)**.
[28] M.I.Vinnik, Yu.V.Moiseev; Izv.Akad.Nauk SSSR, Ser.Khim., **4**, 777 **(1983)**.
[29] M.I.Vinnik, S.A.Skakun, I.G.Tribrat; Kinet.Katal., **31**, 35 **(1990)**.
[30] M.I.Vinnik, P.A.Obraztsov; Kinet.Katal., **19**, 239 **(1978)**.
[31] P.A.Obraztsov, M.I.Vinnik; Kinet.Katal., **19**, 1344 **(1978)**.
[32] Alfred T.Blomquist, (Ed.); 'Organic Chemistry. A series of monographs', v.17: C.H.Rochester; Acidity functions Academic Press, London and New York, **(1970)**.
[33] I.S.Kislina, T.K.Rodima, M.I.Vinnic, L.G.Bushmakin; Izv.Akad.Nauk SSSR Ser.Khim., **1**, 35 **(1990)**.
[34] G.I.Miculine; 'Physical-chemical aspects of electrolyte solutions,' Chemistry, Leningrad, **(1968)**.
[35] R.A.Robinson, R.H.Stokes; 'Electrolyte solutions,' Butterworth scientificpublications, London, **(1965)**.
[36] C.D.Johnson, A.R.Katritzky, S.A.Shapiro; J.Am. Chem.Soc., **19**, 6654 **(1969)**.
[37] E.M.Arnett, G.W.Mach; J.Am.Chem.Soc., **20**, 1177 **(1966)**.
[38] E.M.Arnett, G.W.Mach; J.Am.Chem.Soc., **5**, 2671 **(1964)**.